Reversing the motion analyzed at this point, one obtains a spherical screwlike vortex filled by a viscous fluid and moving in a straight line in a frictionless fluid, steady at infinity, with the velocity $w_0 \exp \times (-b^2\nu t/a^2)$ in the direction of the z axis.

The reaction of the fluid to this vortex in the projection onto the direction of its motion is

$$R_z = \frac{2}{3} b^2 \pi a \mu w_0 \exp(-b^2 \nu t/a^2).$$

This force decreases in the course of time the more rapidly, the smaller the vortex radius and the greater the viscosity of the fluid filling it.

LITERATURE CITED

1. V. A. Steklov, "A case of motion of a viscous incompressible fluid," Soobshch. Khar'kovsk. Mat. Obshch., Ser. 2, 5 (1896).
2. L. M. Milne-Thomson, "Axisymmetrical isovistive flows with vorticity proportional to distance from the axis," Rev. Roum. Sci. Techn. Mec. Appl., 13, No. 6 (1968).
3. Current State of Hydroaerodynamics of Viscous Fluids [Russian translation], Vol. 1, IL, Moscow (1948).
4. O. F. Vasil'ev, Principles of Mechanics of Screwlike and Circulation Flows [in Russian], Gosénergoizdat, Moscow–Leningrad (1958).
5. N. I. Alekseev, "Gromeck flow for incompressible viscous fluid," Nauchn. Zap. Mosk. Gidromeliorat. Inst. im. V. R. Williams, 17 (1948).
6. G. K. Batchelor, An Introduction to Fluid Dynamics, Cambridge University Press (1967).
7. A. G. Yarmitskii, "A three-dimensional analog of a Chaplygin rotational column (generalized Hill vortex)," Zh. Prikl. Mekh. Tekh. Fiz., No. 5 (1974).

DIFFUSION OF POLYMER SOLUTIONS IN A TURBULENT BOUNDARY LAYER

A. V. Vdovin and A. V. Smol'yakov

UDC 532.526

In the last 10 years much progress has been made with the experimental investigation of the Toms effect – the reduced friction in turbulent flows containing small amounts of high-molecular-weight compounds (polymers). However, most experiments have been made at a constant polymer concentration, e.g., in connection with the flow of previously prepared solutions through pipes and channels. Much less attention has been paid to the more complicated but very important practical situation in which a polymer is introduced into a turbulent boundary layer (TBL) through a surface slit. In this case, as a result of turbulent diffusion, the polymer concentration falls off both downstream from the slit and in a direction normal to the surface. On the one hand, the diffusion of the polymer depends on the turbulent mixing capability of the flow, while, on the other hand, it directly affects that capability. This explains why the diffusion of active admixtures in turbulent flows is more complicated and has been less studied than that of passive admixtures that do not affect the flow.

Qualitatively, for both active and passive admixtures, the diffusion process in TBL is characterized by the existence of three zones along the flow. In the initial zone, nearest to the slit source, the admixture diffuses from the wall to the outer edge of the viscous sublayer. In the following intermediate zone the admixture progressively occupies the whole of the TBL and the thickness of the diffusion layer approaches the thickness of the dynamic layer. This stage is followed by diffusion in the end zone.

For both active and passive admixtures the initial zone is very short and at $q \geq 50\nu$ it is totally absent (q is the solution flow rate per unit length of the slit and ν is the kinematic viscosity of the flow, so that the right side of the inequality is the flow rate in the viscous sublayer). For passive admixtures the intermediate zone is also small (about 60-80 TBL thicknesses) [1]. Accordingly, in the diffusion calculations for passive admixtures it is usual to ignore the presence of the first two zones and take into account only the third, most

Leningrad. Translated from Zhurnal Prikladnoi Mekhaniki i Tekhnicheskoi Fiziki, No. 2, pp. 66-73, March-April, 1978. Original article submitted February 17, 1977.

0021-8944/78/1902-0196 $07.50

extensive end zone [2]. This is convenient as well as justified, since the end zone is characterized by simple asymptotic relations.

In the end zone the concentration of active admixtures is usually low and their action on the flow gradually diminishes as the x coordinate increases. Accordingly, for active admixtures, too, the end zone is the simplest and to a large extent resembles the end zone for passive admixtures. Evidently, this is why students of the Toms effect take only the end zone into account [3, 4]. As in the case of passive admixtures, this is convenient but, unfortunately, only partly justified owing to the lack of reliable experimental data on polymer diffusion in the intermediate zone. Our measurements have shown that for polymers the intermediate zone is much longer than for passive admixtures and for that reason alone should not be neglected. Moreover, it is precisely in the intermediate zone that the hydrodynamic effects are greatest owing to the high concentration of polymer in the wall zone of the TBL where the polymer is known to exert its main influence on the turbulence.

Accordingly, we will concentrate our attention on the intermediate polymer solution diffusion zone. We have measured the concentration of active (WSR-301 polyethylene oxide) and passive (potassium chloride KCl) admixtures diffusing in the TBL on a flat plate from a line source (surface slit) at right angles to the flow. The results of the measurements are presented below.

The TBL was developed on the flat wall of the working section of a hydrodynamic test channel 150 × 75 mm in cross section and 1000 mm long. The admixture concentration was measured at distances x = 157, 357, and 557 mm from the source at a minimum step along the normal to the wall $\Delta y = 0.1$ mm. The ranges of variation of the experimentally controlled quantities were as follows: for the flow velocity u_∞ at the outer edge of the TBL from 2 to 12 m/sec; for the Reynolds numbers Re* (displacement thickness) from $6 \cdot 10^3$ to $2 \cdot 10^4$; for the specific (per unit length of source) solution flow rates q from 0.083 to 12.5 cm^2/sec; for the initial concentration c_0 of the solution introduced into the flow through the slit from $5 \cdot 10^{-4}$ to $5 \cdot 10^{-3}$ g/cm^3.

The slit was designed to ensure that the solution was injected in a direction almost tangential to the wall. The cross section of the slit measured 0.7 × 120 mm and the solution was injected by means of compressed air. The flow rate was measured with rotameters. The distribution of the diffusing admixture in the TBL was investigated by sampling the flow at various points and then measuring the concentration in the samples with a specially designed instrument – a polarograph capable of determining concentrations of 10^{-6} g/cm^3 or more [5]. The wall samples were taken through taps 0.5 mm in diameter and the flow samples by means of microsampling tubes with an orifice measuring 0.15 × 1.5 mm.

Figure 1 shows the decrease in the wall concentration c_w downstream from the source for a passive admixture KCl (curve 1) and an active polymer WSR-301 (curve 2). Clearly, the KCl concentration falls very rapidly (in approximately inverse proportion to the distance from the source), which is fully consistent with the known data [1, 2]. Under the same conditions the polymer concentration decreases much more slowly. This is because polymers substantially reduce the turbulent mixing. If we introduce the longitudinal diffusion scale factor L by means of the relation $c_w(L) = c_0 e^{-1}$, where c_0 is the initial concentration of the solution on leaving the slit, then, as follows from Fig. 1, the value of L turns out to be 15-20 times greater for WSR-301 than for KCl.

In Fig. 2 we have plotted the results of measuring the dimensionless wall concentration c_w / c_0 against the dimensionless distance x / L (curve 2 for WSR-301 lies to the left of curve 1 for KCl as a result of the above-mentioned sharp difference in L values). The various points on curve 2 relate to different combinations of distances from the source (x = 157, 357, and 557 mm), flow velocities (u_∞ = 4.8 and 12 m/sec), and solution flow rates (q = 0.85, 1.7, 2.12, 2.96, 8.5, 8.75 cm^2/sec). The initial concentration was $1.12 \cdot 10^{-3}$ g/cm^3. Clearly, the law of decrease in wall concentration for active admixtures is essentially different from the hyperbolic law for passive admixtures: at $0 < x/L < 6$ it is close to exponential

$$c_w/c_0 = \exp(-\alpha x/L - \beta), \quad (1)$$

where for WSR-301 solutions $\alpha = 0.7$ and $\beta = 0.3$.

In order to be able to use relation (1) or the data for Fig. 2 it is necessary to know how the scale factor L varies with variation of the conditions of solution injection and the flow conditions in the TBL. In Fig. 3 we have plotted the results for flow velocities of 2, 4, and 8 m/sec, polymer flow rates of 0.85, 2.12, 4.23, and 8.5 cm^2/sec, and starting solution concentrations of $0.56 \cdot 10^{-3}$, $1.12 \cdot 10^{-3}$, $2.24 \cdot 10^{-3}$, $5 \cdot 10^{-3}$ g/cm^3.

These data show that L depends not on q and c_0 taken separately but on their product qc_0, i.e., on the resultant amount of polymer injected into the flow per unit time. This dependence is such that at small qc_0

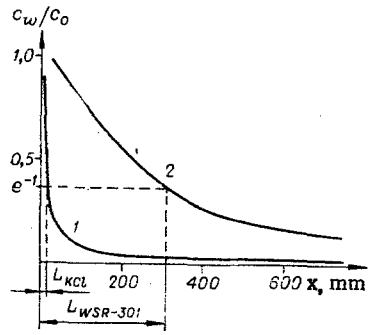

Fig. 1

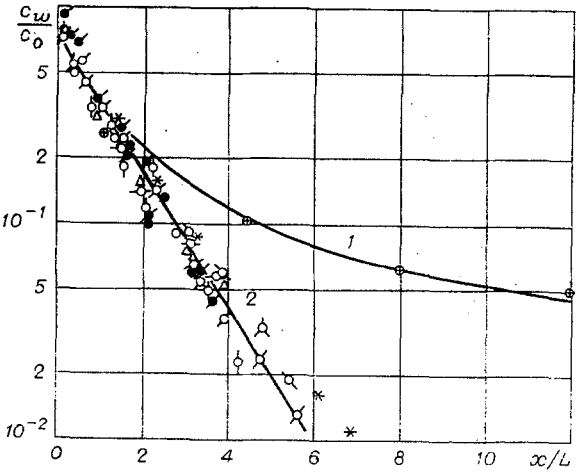

Fig. 2

the scale factor L is approximately proportional to qc_0, while at large qc_0 it is almost independent of the latter. Clearly, at high qc_0 there is more than enough polymer to saturate the wall zone and the "excess" polymer diffuses into the outer part of the TBL without increasing the concentration near the wall.

An interesting feature of these wall data is the fact that they do not depend on u_∞ and hence on the turbulent diffusion rate in the outer part of the TBL. This is radically different from the situation for passive admixtures, where c_w is inversely proportional to u_∞. The conservativeness of the polymer diffusion processes in the immediate vicinity of the wall in relation to the turbulent mixing in the outer part of the TBL is attributable to the almost total suppression by the polymer of the turbulent fluctuations at the wall. Under these conditions the viscous sublayer may be regarded as almost laminar, which, of course, is not true of the ordinary viscous sublayer with its fairly intense velocity fluctuations, which have a marked effect on the transfer processes [6].

It is natural to assume that in the laminar viscous sublayer the diffusion of the active admixture does not depend on the turbulence in the parts of the TBL further from the wall and accordingly is determined solely by the physical properties of the transporting medium, its flow rate in the region in question, and the transportability of the diffusing polymer particles. The properties of the medium are characterized by its kinematic viscosity ν and density ρ. The flow rate in the viscous sublayer depends only on the viscosity, $q_{VS} = a^2\nu/2$, where a is the local Reynolds number of the sublayer (of the order of 10). From the theory of Brownian motion it follows that the transportability of diffusing particles in a given medium is uniquely described by the characteristic dimension of the particles h.

Hence, the process is determined by the parameters ν, ρ, and h. From these it is possible to construct a unique dimensionless combination for the argument of the longitudinal diffusion scale factor: qc_0/μ ($\mu = \rho\nu$ is the dynamic viscosity of the solvent), as shown in Fig. 3. The dimensionless representation of the diffusion scale factor itself takes the form L/h. A possibly more convenient form is $L\mu D/kT$, which follows from the expression $D = kT/6\pi\mu h$ relating the molecular diffusion coefficient D with the dimension h of the diffusing particles, the viscosity μ, and the temperature T of the medium (k is Boltzmann's constant).

At the moment, the values of D and h for polymer particles are not known with sufficient accuracy; accordingly, in Fig. 3, L is given in dimensional form; curve 1 relates to freshly prepared WSR-301 solutions and curve 2 to WSR-301 solutions kept for 5 days prior to the experiment at a concentration of 10^{-3} g/cm^3. During this period there was either partial chemical degradation of the macromolecules or some further dissolving of the supermolecular formations. As a result, the hydrodynamic efficiency of the solution was somewhat reduced, together with the characteristic particle dimension, and the diffusion coefficient correspondingly increased. It may therefore be assumed that the dimensionless function $L\mu D/kT = \varphi(qc_0/\mu)$ could have combined curves 1 and 2 in Fig. 3. Later on it would be useful to see whether this function is a universal one applicable to all drag-reducing polymers.

Examples of the distribution across the TBL of the dimensional concentration of the WSR-301 solution in the intermediate zone are given in Fig. 4. It was found that the concentration distribution in the TBL (except for a small wall zone) is determined by the parameter $qc_0/\rho u_\infty x$ and the data in Fig. 4 correspond to a value for this parameter of $2.1 \cdot 10^{-7}$. The parameter is a ratio of two parameters:

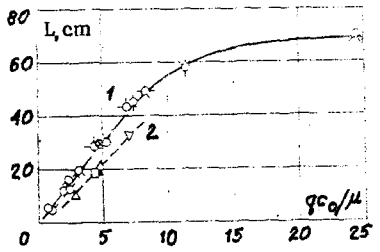

Fig. 3

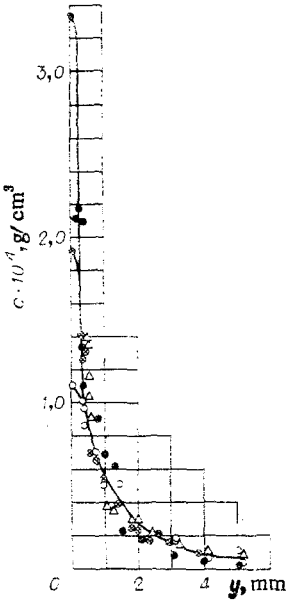

Fig. 4

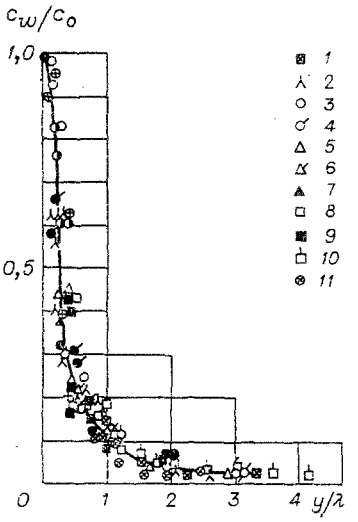

Fig. 5

$$\frac{qc_0}{\rho u_\infty x} = \frac{qc_0}{\mu}\Big/\frac{u_\infty x}{\nu},$$

and it follows from Figs. 3 and 4 that whereas near the wall only the dimensionless flow rate qc_0/μ is decisive, in the outer part of the TBL the Reynolds number $u_\infty x/\nu$ also plays a role. Thus, for a polymer admixture in the intermediate zone of the TBL it is possible to distinguish two characteristic regions (a conservative wall region and an outer region), whereas for passive admixtures the concentration distribution is determined up to the wall by the single parameter $qc_0/\rho u_\infty x^m$, where m is close to unity [1].

The family of curves $c = f_1(y)$ with parameter $qc_0/\rho u_\infty x$ for the outer part of the TBL (see Fig. 4) can be represented in the form of a single dimensionless curve $c/c_w = f_2(y/\lambda)$, where λ is a certain conventional thickness of the diffusion layer (Fig. 5; for the variation of the parameters see Table 1). From this there follows

$$c_w = \frac{c}{f_2(y/\lambda)} = \frac{f_1(y)}{f_2(y/\lambda)}.$$

However, by definition, the wall concentration c_w cannot depend on the y coordinate. Consequently, the function f_1 must enter into function f_2 as a cofactor: $f_2(y/\lambda) = f_1(y)f(\lambda)$, and this is only possible if f_2 is an exponential function. Thus,

$$f_2(y/\lambda) = A(y/\lambda)^n = (By^n)\left(\frac{A}{B}\lambda^n\right), \tag{2}$$

where A depends on the method of determining the diffusion thickness of the layer λ and for the method adopted in this case $c(\lambda) = 0.1c_w$ we have A = 0.1. It is also clear that the first factor on the right side of (2) represents $f_1(y)$ with coefficient B depending on $qc_0/\rho u_\infty x$. Thus, the two functions shown in Figs. 4 and 5 must both take the form of a power dependence. Figure 6, plotted to a log–log scale using the data of Fig. 5, clearly shows that for $n \approx -4/3$ and A = 0.1 relation (2) is closely satisfied on an interval of distances from the wall of approximately four octaves. Exceptions are the wall zone of the TBL and possibly its outermost parts.

The beginning of the end diffusion zone corresponds to the merging of the diffusion and dynamic boundary layers. Accordingly, we take the thickness δ of the latter as the characteristic length scale factor of the former:

$$c/c_w = f_3(y/\delta). \tag{3}$$

In the end zone it is possible to express the total flow rate of the diffusing admixture in terms of function (3) and the mean velocity profile $u/u_\infty = g(y/\delta)$:

$$qc_0 = \int_0^\infty cu\,dy = c_w\delta u_\infty\gamma,$$

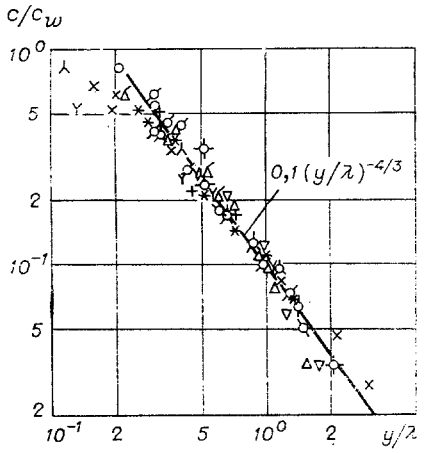

Fig. 6

TABLE 1

Polyethylene oxide WSR-301, $c_0 = 1{,}12 \cdot 10^{-3}$ g/cm³			
No. of points in Fig. 5	q, cm²/sec	u_∞, m/sec	x, mm
1	4,23	8	157
2	12,1	12	157
3	2,12	4	357
4	4,32	4	357
5	4,23	8	357
6	6,27	8	357
7	8,57	8	357
8	6,60	12	357
9	12,1	12	357
10	2,12	4	557
11	4,23	4	557

where

$$\gamma = \int_0^\infty f_3(y/\delta)\, g(y/\delta)\, d(y/\delta).$$

The parameter $\gamma = \bar{c}/c_W$ characterizes the concentration averaged over the cross section of the TBL $\bar{c} = qc_0/\delta u_\infty$ normalized to the wall concentration c_W. It also indicates the uniformity of the transverse concentration distribution. For homogeneous solution $\gamma = 1$; when the solution is introduced through a surface slit $\gamma < 1$, since the maximum concentration occurs at the wall. Because turbulent diffusion equalizes the concentration distribution, the coefficient γ increases downstream from the source, which indicates that the wall concentration c_W decreases more rapidly than the mean concentration $\bar{c}$.

The uniformity coefficient for passive admixture reaches a maximum value $\gamma \approx 0.55$ at the end of the intermediate zone, remaining constant in the end zone. For polymers, whose localization in the conservative wall zone is quite high, it is usual to observe $\gamma < 0.55$ in the initial part of the end zone, where the Toms effect is still in evidence. This occurs at large values of qc_0/μ when the longitudinal diffusion scale factor L is close to its maximum. In this case L depends only slightly on qc_0/μ (see Fig. 3) and for the uniformity coefficient, using (1), we can write

$$\gamma = \frac{qc_0}{\delta u_\infty c_w} = \frac{q}{\delta u_\infty} \exp\left(\alpha \frac{x}{L} + \beta\right) = \frac{q}{Q}\left(1 - \frac{\delta^*}{\delta}\right) \exp\left(\alpha \frac{x}{L} + \beta\right), \tag{4}$$

where δ^* is the displacement thickness of the TBL; Q is the flow rate through the TBL, which is related with the product $u_\infty \delta$ as follows:

$$Q = u_\infty\, \delta(1 - \delta^*/\delta).$$

The uniformity coefficient γ is the greater, the greater the ratio of the flow rate of the polymer solution q to the net flow rate Q in the TBL. However, as noted above, for a slit source γ never exceeds about 0.55, and for polymer solutions the transition from (4) to a constant value occurs the sooner, the smaller the longitudinal diffusion scale factor L. In our experiments, even at maximum values, it was not possible to obtain values of γ lower than 0.42-0.45 for polymers in the end diffusion zone, which is only 20-30% less than the asymptotic value of 0.55. At small values of qc_0/μ, when the longitudinal diffusion scale factor L is also small (see Fig. 3), $\gamma \approx 0.55$ was observed from the very beginning of the end zone.

LITERATURE CITED

1. M. Poreh and J. E. Cermak, "Study of diffusion from a line source in a turbulent boundary layer," Intern. J. Heat Mass Transfer, 7, No. 10, 1083-1095 (1964).
2. A. S. Monin and A. M. Yaglom, Statistical Hydromechanics [in Russian], Part 1, Nauka, Moscow (1965).
3. A. G. Fabula and T. J. Burns, "Dilution in a turbulent boundary layer with polymeric friction reductions," Naval Undersea Research and Development Center, Pasadena, Cal., TP 171 (1970).
4. V. A. Ioselevich and V. N. Pilipenko, "Drag of a flat plate in a polymer solution flow of variable concentration," Izv. Akad. Nauk SSSR, Mekh. Zhidk. Gaza, No. 1 (1974).

5. A. V. Vdovin, "Diffusion of polymers from a line source in a turbulent boundary layer," in: Abstracts of Proceedings of the 24th All-Union Scientific-Technical Conference on Ship Theory [in Russian], Sudostroenie, Leningrad (1975).
6. E. M. Khabakhpasheva, "Some data on the flow structure in a viscous sublayer," in: Problems of Thermophysics and Physical Hydrodynamics [in Russian], Nauka, Novosibirsk (1974).

EXPERIMENTAL INVESTIGATION OF THE INTERACTION OF COLLIDING DROPLETS

V. A. Arkhipov, G. S. Ratanov, and V. F. Trofimov

UDC 532.529

Information concerning the coalescence and disruption of colliding droplets is needed for solving a number of problems of two-phase flow dynamics. A considerable number of studies have been devoted to droplet collision [1-8]; so far, however, in calculating flows with allowance for particle coagulation and disruption, approximate hypotheses and empirical formulas for the droplet coalescence probability have been used. Below we present the results of a cinematographic investigation of the collision of free-flying droplets in air. As distinct from the authors of [2, 3], we investigated not averaged mass collision effects, but the behavior of individual interacting droplets in relation to the criteria determining the result of the collision.

The apparatus consisted of two generators producing continuous counterflows of monodisperse droplets which we shall agree to call targets (the larger-diameter droplets) and projectiles. In order to obtain target droplets $(0.6\text{-}1.2) \cdot 10^{-3}$ m in diameter we used a generator of the "vibrating capillary" type in which vibrations with a frequency of 20-100 Hz were produced by an electrodynamic transducer. Projectile droplets $(0.3\text{-}0.8) \cdot 10^{-3}$ m in diameter were obtained in a generator of the "rotating capillary" type. Liquid from a tank mounted on the shaft was supplied to the capillary through an intermediate tube. On rotation, a droplet was cut off by a metal thread $50 \cdot 10^{-6}$ m in diameter placed near the end of the capillary at right angles to the plane of rotation. This ensured the separation of droplets at a certain point on the periphery at a frequency of 5-200 droplets per second. The droplet collision velocity $u = 1\text{-}5$ m/sec. The collision process was recorded with an SKS-1M high-speed motion-picture camera at the rate of 1500-3000 frames per second. The experiments were conducted with distilled water [whose density, dynamic viscosity, and surface tension were, respectively, $\rho = 10^3$ kg/m^3, $\eta = 10^{-3}$ kg/(m·sec), and $\sigma = 72.88 \cdot 10^{-3}$ kg/sec^2 at a temperature of +20°C].

The interaction of droplets with a given diameter ratio (in our experiments $\gamma = D_2/D_1 = 1.9 \pm 0.8$) is determined by the collision angle θ (the angle between the droplet collision velocity vector and the straight line connecting the centers of the droplets at the moment of contact) and the Weber number $W = \rho u^2 D_1/\sigma$. For water droplets the viscosity forces are negligibly small compared to the surface tension and inertia forces; accordingly, the effect of the criterion containing η (for example, $Lp = \rho\sigma D_2/\eta^2 \sim 10^5$) is unimportant. Under our experimental conditions the value of θ was not determined, and the results obtained represent averages over all possible values of the collision angle $\theta = 0 - \pi/2$. On the interval $W = 0.1\text{-}120$ qualitatively different types of interaction were observed, depending on the value of the Weber number.

1. At $0 < W < 0.5$ we observed coalescence of the droplets under the influence of surface tension forces (Fig. 1a). The interactions at small values of W were obtained as a result of droplets from the same generator overtaking each other. Droplet coalescence at low collision velocities can be attributed to vibration of the surface of the droplets and a reduction of pressure in the gap between them [7] or to saturation of the atmosphere with vapor [1, 6]; however, there is no generally accepted opinion on this point.

2. In collisions at W from 0.7 to 1.5 the projectile droplet was observed to rebound from the target droplet (see Fig. 1b). The probable cause of rebound is the presence of an intervening gas layer between the droplets [1, 7]. It may be assumed that the impact of the colliding droplets is insufficient to displace the gas and achieve physical contact. In [8] rebound is attributed to the elastic properties of the surface layer of the droplets; coalescence is possible only after considerable deformation of the droplets, when the kinetic collision energy is comparable with the free surface energy. This assumption is contradicted, however, by the observed

Tomsk. Translated from Zhurnal Prikladnoi Mekhaniki i Tekhnicheskoi Fiziki, No. 2, pp. 73-77, March-April, 1978. Original article submitted March 10, 1977.

0021-8944/78/1902-0201 $07.50